THE AMERICAN SOCIETY OF MECHANICAL ENGINEERS
345 E. 47th St., New York, N.Y. 10017

96-GT-141

IGV-ROTOR INTERACTION ANALYSIS IN A TRANSONIC COMPRESSOR USING THE NAVIER-STOKES EQUATIONS

Andrea Arnone
"Sergio Stecco" Department of Energy Engineering
University of Florence
Florence
Italy

Roberto Pacciani
Nuovo Pignone S.p.A.
Florence, Italy

ABSTRACT

A recently developed, time-accurate multigrid viscous solver has been extended to handle quasi-three-dimensional effects and applied to the first stage of a modern transonic compressor. Interest is focused on the inlet guide vane (IGV):rotor interaction where strong sources of unsteadiness are to be expected. Several calculations have been performed to predict the stage operating characteristics. Flow structures at various mass flow rates, from choke to near stall, are presented and discussed. Comparisons between unsteady and steady pitch-averaged results are also included in order to obtain indications about the capabilities of steady, multi-row analyses.

INTRODUCTION

The real flow inside a turbine or compressor is unsteady and strongly influenced by the interaction of pressure waves, shock waves, and wakes between stators and rotors. Three-dimensional, time-accurate simulations of viscous flows are yet to come for practical design purposes. However, designers are trying to arrive at a better comprehension of the multistage environment in order to further increase machine performance.

Unsteady calculations provide realistic simulations which allow one to gain more insights into the flow physics of component interactions. Moreover, they can be used as target solutions for fine-tuning steady multi-row pitch-averaging techniques. The works of Erdos et al. (1977), Rai (1987), Lewis et al. (1987), Jorgenson and Chima (1988), Giles (1988a), and Rao et al. (1992) are some examples of basic historical contributions to this topic.

A multigrid Navier-Stokes time accurate solver (TRAF, Arnone et al. 1993) has recently been extended to the analysis of unsteady rotor-stator interaction. The computational procedure uses fully implicit time discretization. A four-stage Runge-Kutta scheme is used in conjunction with several accelerating techniques typical of steady-state solvers instead of traditional time-expensive factorizations. The capability of the procedure was previously investigated by applying it to a gas turbine stage. In this phase, particular attention was dedicated to grid dependency in space and time as well as to the influence of the number of blades included in the calculation (Arnone et al. 1994, 1995)

In this paper, a quasi-three-dimensional release of the TRAF code has been developed and applied to the first stage of a modern transonic compressor. The analysis has been restricted to the inlet guide vanes (IGV):rotor interaction where most of the unsteadiness is to be expected. Several mass flow rates, from choke to near stall, have been analyzed in order to reproduce the stage operating characteristic. The main flow features at various operating conditions are presented and discussed.

Time-averaged results have been compared to steady, pitch-averaged ones. The effects of spurious shock reflections have been investigated by comparing a non-reflective procedure (Giles, 1988a, 1988b) with simple one-dimensional, characteristic boundary treatment. The relative merits of different pitch-wise averaging are also discussed.

It has been found that the reflective properties of the boundary conditions represent the first problem which needs to be overcome to obtain reliable steady multistage calculations. Once this problem is addressed, good agreement between time- and pitch-averaged results can be achieved.

Presented at the International Gas Turbine and Aeroengine Congress & Exhibition
Birmingham, UK — June 10-13, 1996
This paper has been accepted for publication in the Transactions of the ASME
Discussion of it will be accepted at ASME Headquarters until September 30, 1996

GOVERNING EQUATIONS AND TURBULENCE MODEL

The time-accurate release of the TRAF code (Arnone, 1993, Arnone et al., 1994, 1995) has been extended to handle quasi-3D effects. The unsteady, Reynolds-averaged Navier-Stokes equations have been formulated for an axysimmetric blade-to-blade surface and accounts for both radius and streamtube thickness variations. The governing equations are written in conservative form in a curvilinear, body-fitted coordinate system and solved for density, absolute momentum components in the axial and tangential directions, and total energy (e.g. Jorgenson and Chima, 1988).

A two-layer algebraic model based on the mixing length concept is used for turbulence closure. In the near wall region the mixing length is computed using the Prandtl-Van Driest formula while in the outer region and on the wake it is kept constant to a fixed fraction of the shear layer thickness δ, according to the standard relation (e.g. Kwon et al., 1988, Vuillot et al., 1993):

$$\ell_{outer} = 0.085\delta$$

First attempts to determine the outer length scale using methods derived from the Baldwin-Lomax (1978) and Chima, Giel and Boyle (1993) models have led to unsatisfactory results in transonic compressors. For those configurations large regions with unrealistically high mixing length values and eddy viscosity were noticed. In the rotor row of a transonic compressor, vorticity may be large, even away from the blade boundary layer due to strong shock systems and incoming wakes from the stator row. In such a situation the vorticity may not decay rapidly away from the wall. As a consequence, the models considered failed to predict a reasonable outer length scale distribution on the blade surface. Valkov and Tan (1995) observed a similar situation in wake-blade interaction computations and proposed a suitable modification of the Baldwin-Lomax model in order to address the problem. In the present work, an algebraic criterium, which resembles the features of both the Baldwin-Lomax (1978) and Chima, Giel and Boyle (1993) models, but which implicitly introduces a cut-off criterium for the vorticity field based on the distance from the wall, is used to estimate the boundary layer thickness. If y denotes the distance normal to the wall, ω the vorticity magnitude, and D the Van-Driest damping factor, the value y_{max} at which the function:

$$G(y) = \frac{1}{y}\int_0^y y\omega D dy \qquad (1)$$

reaches its maximum is assumed as a turbulent length scale. The boundary layer thickness is then obtained from the relationship:

$$\delta = 1.145 y_{max} \qquad (2)$$

which arises from adoption of the Coles wall-wake law to represent turbulent velocity profiles (e.g. Chima et al, 1993, Stock et al., 1987). The proposed model has been assessed in various turbine and compressor configurations and it has proven to be quite effective for steady as well unsteady analyses. The function $G(y)$ can ideally have spurious peaks at grid locations far from the wall but its absolute maximum has always been found to occur in the outer part of the blade boundary layer leading to reliable estimates of the mixing length.

SPATIAL DISCRETIZATION AND ARTIFICIAL DISSIPATION

The space discretization is based on a cell-centered finite volume scheme. On each cell boundary, fluxes are calculated after computing the necessary flow quantities at the center of the side. Those quantities are obtained by a simple averaging of adjacent cell-center values of the dependent variables.

The artificial dissipation model used in this paper is basically the one originally introduced by Jameson, Schmidt, and Turkel (1981). In order to minimize the amount of artificial diffusion inside the shear layer, the eigenvalues scaling of Martinelli and Jameson (1988), and Swanson and Turkel (1987) have been implemented to weight these terms (e.g. Arnone and Swanson, 1993).

BOUNDARY CONDITIONS

In cascade-like configurations, there are four different types of boundaries: inlet, outlet, solid wall, and periodicity. In the case of a multistage environment, more than one blade row is taken into consideration, and inlet and outlet refer to the first row inlet and last row exit, while the link between rows must be provided by means of some technique.

According to the theory of characteristics, the flow angle, total pressure, total temperature, and isentropic relations are used at the subsonic-axial first row inlet, while the outgoing Riemann invariant is taken from the interior. At the subsonic-axial last row outlet, the average value of the static pressure is prescribed, and the density and components of velocity are extrapolated.

On the solid walls, the pressure is extrapolated from the interior points, and the no-slip condition and the temperature condition are used to compute density and total energy.

Cell-centered schemes are generally implemented using phantom cells to handle the boundaries. The periodicity is, therefore, easily overimposed by setting periodic phantom cell values. On non-periodic grids (Arnone et al., 1992, Arnone, 1994), the periodic boundaries do not match and the phantom cells overlap the real ones. Linear interpolations are then used to compute the value of the dependent variables.

The link between rows is handled by means of different techniques in steady or unsteady multiblock computations.

In the unsteady case, stator and rotor grids have a common interface line and the match is provided through appropriate calculation of phantom cell values. For the blade passage under

examination, the phantom cells relative to the interface line lie on the adjacent blade passage, and linear interpolations are used to provide the flow variable values. This approach, similar to the one used on periodic boundaries, where grids do not match, is not strictly conservative. However, monitoring of the errors in the conservation of mass, momentum, and energy has indicated a very good level of accuracy. For the practical applications considered up to now, relative errors in conservation were always less then 10^{-4}, which was considered accurate enough.

For steady multi-row computations, different methods to transfer informations from one row to the other have been considered in the present work.

A fairly common method of linking rows can be derived by a characteristic one-dimensional approach where quantities are pitch-averaged at the interface lines and transferred between blocks. Total temperatures, total pressures and flow angles, necessary as inlet conditions, are pitch-averaged on previous blade rows. Static pressures, needed at the outlet boundaries, come from pitch-averaging on successive rows.

Modern state-of-the-art turbine and compressor stages work in transonic regimes and stator and rotors are stacked very close to each other. If inlet and outlet boundaries are located at short distances from the blade rows, the use of the one-dimensional characteristic boundary treatment described above may result in undesired reflections of shock waves (Arnone and Benvenuti, 1994). Moreover, the pitch-averaging process takes place close to the blade passage and, depending on the averaging procedure, the conservation of mass or momentum or energy can be poor if the flow exhibits strong gradients.

One way to overcome such difficulties is to slightly separate the blade rows so that the mixing plane is placed far enough upstream or downstream of the blade rows. Here the flow will result quite uniform in the circumferential direction and the averaging process will be more accurate in conserving mass, momentum and energy. The major disadvantages of this approach arise from its extension to three-dimensions. The bladings of modern compact turbomachines undergo sensible height variation in a single row as well as from row to row in order to accommodate density changes of the flow. As a consequence, endwalls are contoured, and adjustment of the axial gap between rows results in a modification of the meridional channel geometry.

An improved method to deal with the coupling of blade rows in steady multistage calculations, which should allow one to mantain the machine geometry while reducing undesired reflections, is based on the use of non-reflective procedures.

In order to investigate these important issues, the non-reflective treatment proposed by Giles (Giles, 1988a, 1988b) has been used in the present work as an alternative to the one-dimensional characteristic boundary scheme previously discussed. Following this approach, the time variation of each incoming characteristic variable at the inlet and outlet boundaries is decomposed into a sum of a uniform, pitch-averaged part and a tangentially varying fluctuation. The average time variations of incoming characteristics are set in order to match pitch-averaged flow variables at the interface of two rows. The local time variations are treated according to non-reflective conditions derived from a Fourier analysis of linearized, quasi-three-dimensional Euler equations. The outcoming characteristic changes are extrapolated from the interior of the domain.

BASIC MULTIGRID STEADY SOLVER

The system of governing equations is advanced in time using an explicit four-stage Runge-Kutta scheme. A hybrid scheme is implemented, where, for economy, the viscous terms are evaluated only at the first stage and then frozen for the remaining stages (Arnone and Swanson, 1993).

Three techniques are employed to speed up convergence to the steady state-solution: 1) residual smoothing; 2) local time-stepping; and 3) multigrid.

An implicit smoothing of residuals is used to extend the stability limit and the robustness of the basic scheme. The variable coefficient formulations of Martinelli and Jameson (1988), and Swanson and Turkel (1987) are used to obtain effective viscous calculations on highly-stretched meshes (Arnone and Swanson, 1993). The time step is then locally computed on the basis of the maximum allowable Courant number, typically *5.0*, and accounting for both convective and diffusive limitations (Arnone and Swanson, 1993).

The multigrid technique incorporated in the TRAF code is based on the Full Approximation Storage (FAS) schemes of Brandt (1979), and Jameson (1983). A V-type cycle with coarse grid sweeps (subiterations) is used. The turbulent viscosity is evaluated only on the finest grid level and then interpolated on the coarse grids.

On each grid, the boundary conditions are treated in the same way and updated at every Runge-Kutta stage.

MULTIGRID TIME-ACCURATE STEPPING SCHEME

Jameson (1991) proposed a method for the time-accurate integration of the Euler equations using time-marching steady-state techniques. Such an approach has become widely popular since its introduction and it has also been successfully applied to the Reynolds-averaged Navier-Stokes equations (i.e. Arnone et al., 1993, 1994, Alonso et al., 1995). By the introduction of dual time-stepping and a fictitious time, a new residual is defined which includes the real time derivatives of the conservative variables as source terms in addition to the convective, diffusive, and artificial dissipation fluxes. Such derivatives are discretized using a three-point backward formula which results in an implicit scheme which is second-order accurate in time.

Between each time step the solution is advanced in the non-physical time, and acceleration strategies like local time stepping, implicit residual smoothing, and multigridding are used to speed up the new residual to zero to satisfy the time-accurate equations.

The described method has recently been used by the authors to compute the rotor:stator interaction in a transonic gas turbine stage (Arnone et al. 1993, Arnone et al., 1994) and it has indicated up to a *97 %* reduction in the computational effort with respect to classical explicit schemes. By means of the implicit time discretization, stability restrictions are removed, while the efficiency of the explicit approach in addressing high frequency problems can still be maintained by not performing residual smoothing and multigrid. When the characteristic frequency of the problem decreases, accelerating techniques can be gradually introduced to optimize the computational cost.

APPLICATION TO A MODERN TRANSONIC COMPRESSOR STAGE

The quasi-3D release of the TRAF code has been used to study the first stage transonic blading of an axial compressor under development at the Nuovo Pignone Company (Benvenuti, 1996).

A near-tip section of the stage, where the flow is transonic and important unsteady effects are expected, has been selected for the analysis. The streamtube thickness and radius distributions were established on the base of steady, three-dimensional, viscous stage calculations.

In transonic compressors, like the one under consideration, the flow is supersonic in the relative frame at the rotor inlet. It is common in these industrial compressors to have quite a normal passage shock which is detached from the leading edge at nominal conditions. The small axial gap between rows allows the shock wave to enter and to be reflected by the inlet guide vanes. Downstream the rotor throat, the flow is subsonic. Therefore, the unsteady effects experienced by the downstream stator rows are due to pressure waves and wakes from the rotor. Stronger unsteadiness is then to be expected in the inlet guide vanes (IGV): rotor row interaction.

On the base of such considerations, it was decided to restrict the analysis to the IGV:rotor interaction. The entire operating range of the stage (IGV:rotor), from choke to near-stall conditions, was spanned with *9* different mass flow rate values. This extensive analysis was aimed at producing a target solution for the assessment of steady, pitch-averaging techniques as well as to investigate the flow physics of the interaction.

The computational mesh consists of mixed C-type and H-type non-periodic grids. A C-type grid structure (*257x65*) was selected for the IGV. On the contrary, it was found convenient to use an H-type structure (257x161) for the rotor blades. Away from the leading edge, the C-type structure tends to increase the grid size and thus induces a smear of both the incoming wakes and the bow shock. With an H-type structure, it is much easier to control the uniformity and density of the grid before the blade passage. In order to reduce the grid skewness both the C-type and the H-type grids are of the non periodic type (i.e. Arnone et al., 1992, Arnone, 1994).

The presentation of results will be split in two parts. The first section will be used to discuss the unsteady calculations, while the second will be dedicated to the comparison of time-averaged results with the predictions of steady pitch-averaging methods.

Unsteady IGV-Rotor Interaction

The first stage under investigation has *30* inlet guide vanes, *18* rotor blades. The first issue to address is how to account for the ratio between the number of IGV and rotor blades. As mentioned before, the code has been designed to handle more blade passages per each row. Periodic conditions are, therefore, applied only between the first and last block of each row. In our case, assuming steady and uniform inlet and outlet stage boundary conditions, the exact combination would be *5* vanes and *3* rotors.

It is common in an unsteady rotor:stator interaction analysis to limit the number of blade passages included in the calculation in order to end up with reasonable memory and computer time requirements. Inlight of this, an approximate stage configuration including two vanes and one rotor has been considered.

It must be pointed out that the reduction of the number of blocks included in a row produces a pitch alteration which can have an impact on the choke mass flow rate and the flow physics (Arnone et al., 1995). Moreover, an upper limit on the maximum detectable wave length is introduced as,

max. wave length=(blade pitch)x(no. of blades in a row)

This will be reflected in the lowest detectable frequency. For instance, for the rotor row, the lowest detectable frequency will be the one associated with a rotor blade which spans all the inlet guide vanes included in the discretization.

The present stage approximation has been obtained using the exact rotor pitch while slightly reducing the IGV axial chord to preserve solidity. Such an approach allows one to avoid pitch alterations. Unfortunately in three-dimensions, the blade span cannot be adjusted, which results in a modification of the row geometry.

The aspects concerning the limit on the lowest detectable frequency will be discussed later in this section on the basis of a Fourier analysis of the solutions.

A number of *200* temporal divisions within a *cycle* (time that a rotor blade needs to span all the guide vanes included in the discretization) was used. As two vanes are considered in the stage approximation, the time that a rotor blade needs to cross a vane passage (*rotor passing period*) corresponds to *100* time steps.

The non-dimensional blade lift coefficient based on pressure distribution was used to monitor unsteadiness. Previous experience

in unsteady rotor:stator computations (Arnone et al., 1994, 1995) has shown that *100* divisions in a rotor passing period produces a lift evolution which can be considered reasonably independent from the time discretization for practical purposes.

The rotor lift evolution at peak efficiency is reported in fig. 1 as a function of time. The calculations were started from an initial steady-state solution accounting for the rotor blade's motion, but without changing the rotor grid position with respect to the guide vanes. As can be noticed, up to *16* rotor passing periods where needed to obtain a periodic solution. Similar times were needed for the other flow conditions.

Figure 2 summarizes the frequency spectra of the lift evolutions for three different mass flow rate values which refer to choked, peak efficiency, and near stall flow conditions. It can be noticed how the dominant frequencies are equal to or a multiple of the rotor passing one, while only a small amplitude can be observed at frequency which is half the rotor passing one. For choked flow and peak efficiency conditions, the rotor passing frequency is dominating, while near stall the corresponding amplitude has almost completely disappeared with an increase of the one corresponding to half the rotor passing frequency.

At reduced mass flow rates, low frequency phenomena become important. The limit on the lowest detectable frequency introduced by the reduction of the number of blocks does not allow for low frequency phenomena (i.e. rotating stall) to be predicted. Such a limit should not be restrictive away from stall conditions, where high frequencies seems to dominate.

An explanation to the fact that the rotor passing period harmonic disappears as the stage approaches stall, can be attempted assuming that most of the unsteady phenomena are due to the interaction of the leading edge shock with the IGV wakes. Such interaction is depicted in figures 3 and 4, where entropy rise and density contours for choked, peak efficiency, and near stall flow conditions, are reported.

The bow shock interacts with the IGV wake before it is chopped by the passing rotor blades. At high mass flow rates, the wake eventually reaches the passage shock inside the rotor blade channel, once it has been chopped by the rotor blade (choked conditions), or in the throat region (peak efficiency) (fig. 3). Such effects contribute with a frequency which is equal to the rotor passing one.

As stall is approached, the shock/wake interaction mechanism is quite different. While spanning the vane passage, the bow shock pushes the wake, enters the guide vane and is reflected by the IGV blade where a sensible thickening of the boundary layer is visible. As a result of this mechanism, quite a large eddy is formed and convected downstream. As shown in Fig. 3(c) the passage shock interacts with the eddy before it is ingested into the rotor blade passage. Consequently the shock-wake interaction now has two major contributions. One comes from the bow-shock/wake interaction and the other from the passage-shock/eddy interaction. A frequency which is twice the rotor passing one is then expected to dominate. It is worthwhile to notice traces of the described mechanism also in the configuration of the IGV wake at choke and peak efficiency conditions.

At all flow conditions, important harmonics corresponding to multiples of the rotor passing one are present in the lift spectra (Fig. 2). Some explanations for that are listed in the following;

• rotor wake instability is present (fig. 3). Frequency related to wake instability are well above the rotor passing one. At choked condition (fig. 4(a)), the reflection of the passage shock on the rotor suction side has a λ-structure and is located downstream the throat section. As a result of that, a sensible thickening of the blade boundary layer is present on both pressure and suction sides of the rotor blade. It is suspected that such effects are responsible of the evolution of the wake instability in the shedding of vortical spots (fig. 3(a)).

• Although reflections of the bow shock by the guide vanes are much stronger as stall is approached (fig. 4(c)), they can be clearly appreciated even at choked conditions (fig. 4(a), 4(b)). Reflections of this shock by the suction side of the IGV impinges back into the rotor row.

• A rotor blade cuts two IGV wakes in a cycle. The parts of the wakes which are ingested by a rotor row are convected downstream and move with different speeds depending on the compression rate. Pressure and density will increase inside the rotor passage and the motion of these wake parts will progressively lag when decreasing mass flow rate. This situation is quite evident at near-stall conditions (fig. 3(c)), where a large number of eddies chopped from IGV wakes are trapped into the rotor row. Flow unsteadiness related to this phenomenon contributes with frequencies above the rotor passing one.

Steady pitch-averaged analysis

In common industrial practice, it is usual to approach turbomachinery design, by relying on steady predictions. It is then worthwhile to assess how much those predictions can resemble the ones of a realistic, unsteady, multi-row computation.

The comparison between steady and time-averaged predictions has been performed in terms of rotor (mass flow averaged) total pressure ratio and adiabatic efficiency as a function of the flow rate. As usual, the mass flow rates were normalized with their choke value. However, the differences between the various choke flow rates was found to be negligible (less then *0.2 %*).

Figure 5 compares steady rotor row analysis to rotor time-averaged predictions deduced from the stage calculations. Both total pressure ratio (fig. 5(a)) and adiabatic efficiency (fig. 5(b)) are overpredicted in the steady calculations with a slight shift in the peak efficiency point toward lower mass flow rates.

Results for the steady stage-calculation are summarized in figures 6 to 9.

Figure 6 shows predictions obtained using mixing-plane techniques and one-dimensional characteristic treatment for interface boundaries. Pitch-wise mass flow averaging was used to handle mixing planes. In the computations performed with the design row axial gap the total pressure ratio is overestimated (fig. 6(a)) and the adiabatic efficiency (fig. 6(b)) is well above the unsteady one with different shape. Also an important disagreement on the peak efficiency position has to be noticed. Such a situation is known to be a consequence of spurious shock system reflections at the interface boundary (Arnone and Benvenuti, 1994). If the axial gap is increased to *1.25* of the design value, no sensible reflections are experienced and the computed characteristic is very similar to the unsteady one. It is assumed that the bow shock lessens in intensity away from the leading edge. As a consequence, when increasing the axial gap, reflections due to boundary conditions decrease. Note that only the inlet part of the rotor grid was increased to reduce reflections. In such a way the IGV wake mixing losses are the same for the two configurations.

When using non-reflective boundary conditions (fig. 7), the influence of the axial gap is very small. Predicted performance now agrees well with the time-averaged one. The slight differences in the predictions of the two configurations are still the result of weak reflections. The non-reflective procedure used here (Giles, 1988a, 1988b) is based on a linearization of the Euler equations and can produce weak reflections in presence of non-linear phenomena like shock waves.

Figure 8 compares density contours for the time-averaged (fig. 8(a)), non-reflective (fig. 8(b)), and one-dimensional characteristic (fig. 8(c)) treatments. Contours obtained with the non-reflective conditions are close to the time-averaged ones, while the previously mentioned reflections of the one-dimensional characteristic approach are clear in fig. 8(c).

It is worthwhile noticing that the method of linking blade rows by matching mass flow averaged quantities at the interface is not strictly conservative. Despite this fact, all results end up with relative errors in conservation of mass, momentum and energy at the interface of the order of 10^{-4}.

In order to assess the influence of the pitch-wise averaging method, calculations have also been carried out by transferring mixed out parameters between blade rows. These calculations refer to the original configurations and non-reflective boundary conditions. Results are compared to the mass flow pitch-averaged one in fig. 9. The transfer of mixed-out quantities at the interface, instead of mass flow averaged ones, results in a slight decrease in both adiabatic efficiency and total pressure ratio. It is suspected that this is due to the different estimation of the IGV wake losses in the two averaging methods. However, it must be pointed out that the differences arising from different averaging schemes are much smaller than the ones due to spurious reflections (i.e. fig. 6).

Finally it has to be noticed that in the calculations where the influence of reflections are negligible, the agreement in terms of efficiency tends to improve at low mass flow rate. When approaching stall, most of the losses are expected in the strong leading edge shock and unsteady effects seems to reduce their impact. On the contrary, at high flow rates the shock/wake interactions within the rotor row are not accounted for in the steady analysis and the efficiency is overestimated.

CONCLUDING REMARKS

A recently developed quasi-three-dimensional, time-accurate, viscous procedure has been used to study the IGV:rotor interaction in the first stage of a modern transonic compressor. Interaction mechanisms between the rotor shock system and the IGV wakes have been studied for various flow rates.

Unsteady results have been used as a target solution for the comparison with single- and multi-row steady calculations. Spurious shock reflections have been found to produce major discrepancies between unsteady and steady predictions. If the blade rows are slightly separated, reflections are reduced and the use of a simple one-dimensional characteristic treatment leads to good predictions. The non-reflective procedure of Giles (1988a, 1988b) has proven to be effective also for closely stacked rows. It would be interesting to extend this procedure to three-dimensions. A minor impact of the pitch-averaging method has been observed.

ACKNOWLEDGEMENTS

The authors would like to express their gratitude to Prof. Ennio Carnevale and to PIN Engineering for providing computational resources for the project. The authors are also indebted to Nuovo Pignone management and particularly to Drs. Erio Benvenuti, Umberto Corradini, and Bruno Innocenti for the numerous and useful discussions.

REFERENCES

Alonso, J., Martinelli, L., Jameson, A., 1995, "Multigrid Unsteady Navier-Stokes Calculations with Aeroelastic Applications," AIAA Paper 95-0048.

Arnone, A., Pacciani, R., 1995, " Rotor-Stator Interaction Analysis Using the Navier-Stokes Equations and a Multigrid Method," ASME Paper 95-GT-177.

Arnone, A., Pacciani, R., Sestini, A., 1994, "Multigrid Computations of Unsteady Rotor-Stator Interaction using the Navier-Stokes Equations," 1994 ASME Winter Annual Meeting, Chicago.

Arnone, A., 1994, " Viscous Analysis of Three-Dimensional Rotor Flows Using a Multigrid Method, " *Journal of Turbomachinery*, Vol. 116, July 1994, pp. 435-445.

Arnone, A., Benvenuti, E., 1994, "Three-Dimensional Navier-Stokes Analysis of a Two-Stage Gas Turbine, " ASME Paper 94-GT-88.

Arnone, A., Liou, M.-S., and Povinelli, L. A.,1993, " Multigrid Time-Accurate Integration of Navier-Stokes Equations, " AIAA Paper 93-3361-CP..

Arnone, A., Swanson, R. C., 1993, "A Navier-Stokes Solver for Turbomachinery Applications," *Journal of Turbomachinery*, Vol. 115, April 1993, pp. 305-313.

Arnone, A., Liou, M.-S., and Povinelli, L. A.,1992, "Navier-Stokes Solution of Transonic Cascade Flow Using Non-Periodic C-Type Grids, " *Journal of Propulsion and Power*, Vol. 8, No. 2, March-April 1992, pp. 410-417.

Baldwin, B. S., and Lomax, H., 1978, "Thin Layer Approximation and Algebraic Model for Separated Turbulent Flows, " AIAA paper 78-257.

Bevenuti, E., 1996, "Design and Test of a New Axial Compressor for the Nuovo Pignone Heavy Duty Gas Turbines, " accepted for presentation at 1996 ASME TURBO EXPO, Birmingham, UK, June 10-13, 1996.

Brandt, A., 1979, " Multi-Level Adaptive Computations in Fluid Dynamics, " AIAA paper 79-1455.

Chima, R., V., Giel, P., W., Boyle, R., J., 1993, "Algebraic Turbulence Modeling for Three-Dimensional Viscous Flows", proceedings of Engineering Turbulence Modeling and Experiments 2, Florence, 1993

Erdos, J., I., Alzner, E., and McNally, W., 1977, "Numerical Solution of Periodic Transonic Flow Through a Fan Stage," *AIAA Journal*, Vol. 115, No. 11.

Fourmaux, A., Le Meur, A., 1987, "Computation of Unsteady Phenomema in Transonic Turbines and Compressors," 4th Symposium on Unsteady Aerodynamics and Aeroelasticity of Turbomachines and Propellers, Aachen.

Giles, M., B., 1988a, "UNSFLO: A Numerical Method For Unsteady Inviscid Flow in Turbomachinery," GTL Report #195.

Giles, M., B., 1988b, "Non-Reflecting Boundary Conditions for the Euler Equations, "*AIAA Journal*, Vol. 28, No. 12.

He, L., Denton, J., D., 1993, "Three Dimensional Time-Marching Inviscid and Viscous Flow Solutions for Unsteady Flows Around Vibrating Cascades," ASME Paper 93-GT-92.

Jameson, A., 1983, "Transonic Flow Calculations, " MAE Report 1651, MAE Department, Princeton University, July 1983.

Jameson, A., 1991, "Time Dependent Calculations Using Multigrid with Applications to Unsteady Flows Past Airfoils and Wings," AIAA Paper 91-1596.

Jameson, A., Schmidt, W., and Turkel, E., 1981, " Numerical Solutions of the Euler Equations by Finite Volume Methods Using Runge-Kutta Time-Stepping Schemes, " AIAA paper 81-1259.

Jorgenson, P. C. E., and Chima, R., 1988, " An Explicit Runge-Kutta Method for Unsteady Rotor/Stator Interaction", AIAA Paper 88-0049.

Kwon O., K., Pletcher, R., H., Delaney, R., A., 1988, "Calculation of Unsteady Turbulent Boundary Layers, " *Journal of Turbomachinery*, April 1988, Vol. 110, pp. 195-201

Lewis, J. P., Delaney, R. A., Hall, E., J., 1987, "Numerical Prediction of Turbine Vane-Blade Interaction," AIAA Paper 87-21419

Martinelli, L. and Jameson, A., 1988, " Validation of a Multigrid Method for the Reynolds Averaged Equations, " AIAA paper 88-0414.

Rai, M. M., 1987, " Unsteady Three-Dimensional Navier-Stokes Simulations of Turbine Rotor Stator Interactions, " AIAA paper 87-2058.

Rao, K. V., and Delaney, R. A., 1992, " Investigation of Unsteady Flow Through a Transonic Turbine Stage, Part I, Analysis," AIAA paper 90-2408.

Stock, H., W., Haase, W., 1987, "The Determination of Turbulence Length Scales in Algebraic Turbulence Models for Attached as Slightly Separated Flows Using Navier-Stokes Equation, "AIAA paper 87-1302.

Swanson, R. C., and Turkel, E., 1987, " Artificial Dissipation and Central Difference Schemes for the Euler and Navier-Stokes Equations., " AIAA paper 87-1107.

Valkov, T., Tan, C., S., 1995, "Control of the Unsteady Flow in a Stator Blade Row Interacting With Upstream Moving Wakes" *Journal of Turbomachinery*, January 1995, Vol. 117, pp. 97-105

Vuillot, A., M., Couallier, V., Liamis, N. , "3-D Turbomachinery Euler and Navier-Stokes Calculations With a Multidomain Cell-Centered Approach, "AIAA/SAE/ASME/ASEE 29th Joint Propulsion Conference and Exhibit, Monterey, CA, June 28-30, 1993

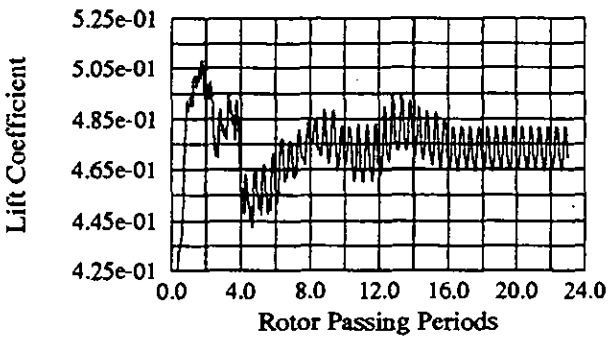

FIG. 1, UNSTEADY ROTOR LIFT EVOLUTION

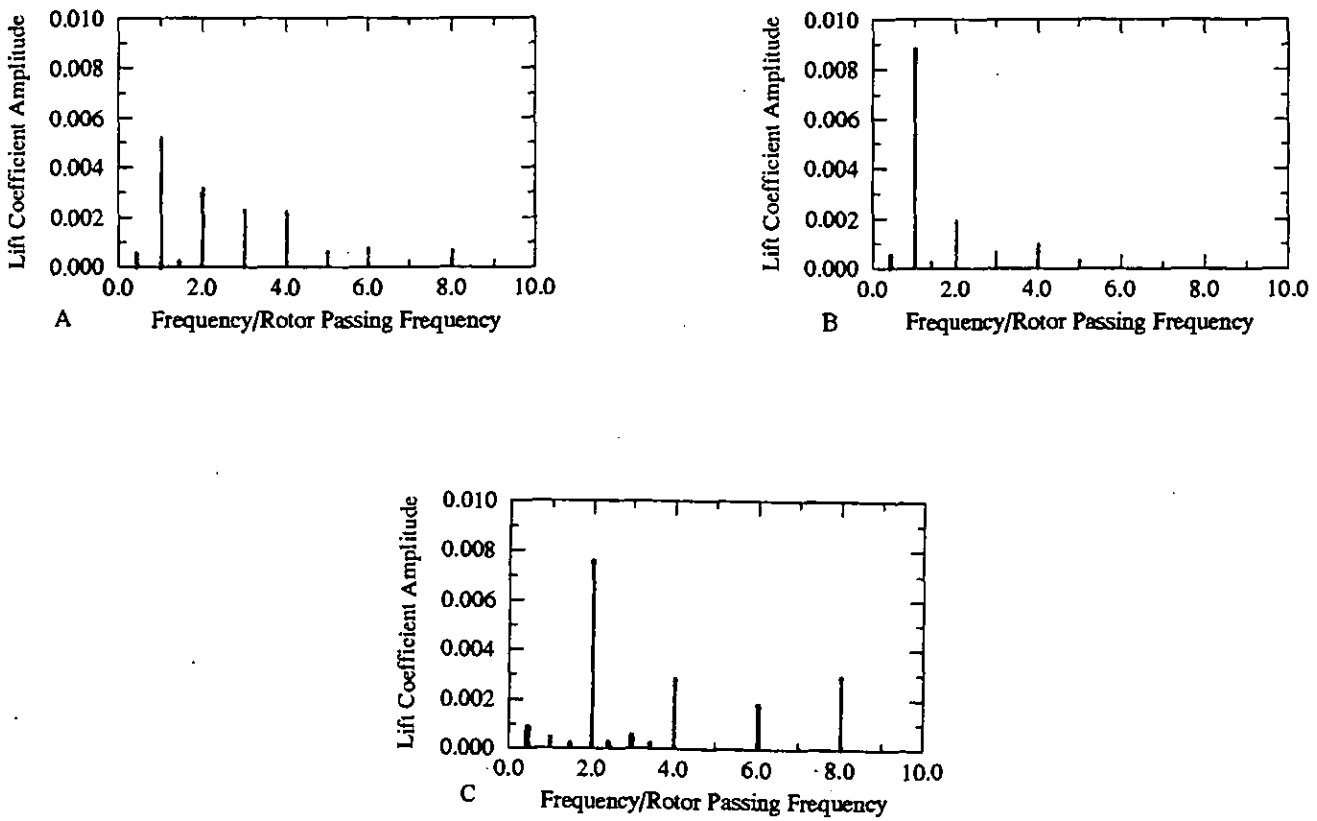

FIG. 2, FREQUENCY SPECTRA OF THE ROTOR LIFT FOR CHOKE (A), PEAK EFFICIENCY (B), AND NEAR-STALL (C) CONDITIONS.

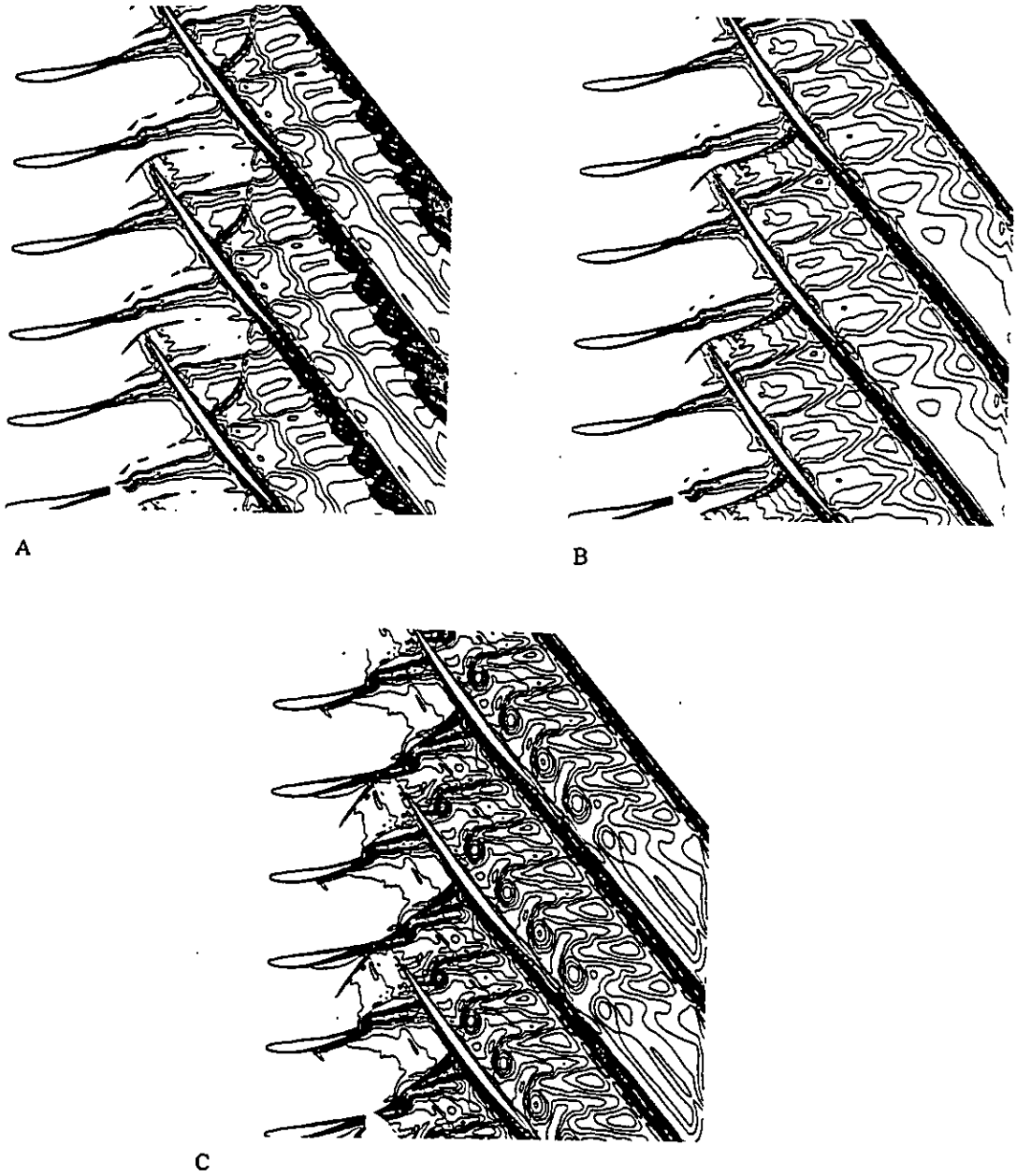

FIG. 3, INSTANTANEOUS ENTROPY RISE CONTOURS FOR CHOKE (A), PEAK EFFICIENCY (B), AND NEAR-STALL (C) CONDITIONS.

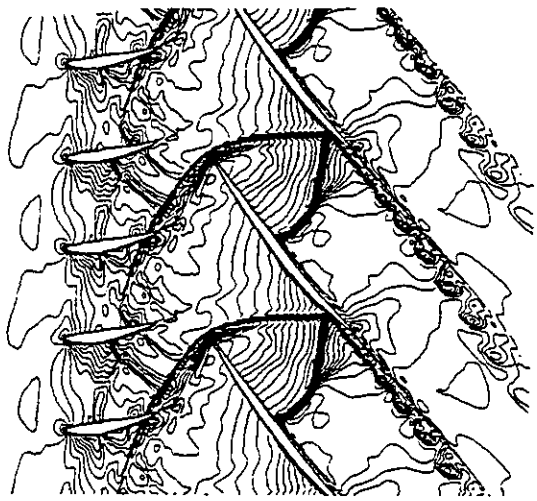

A

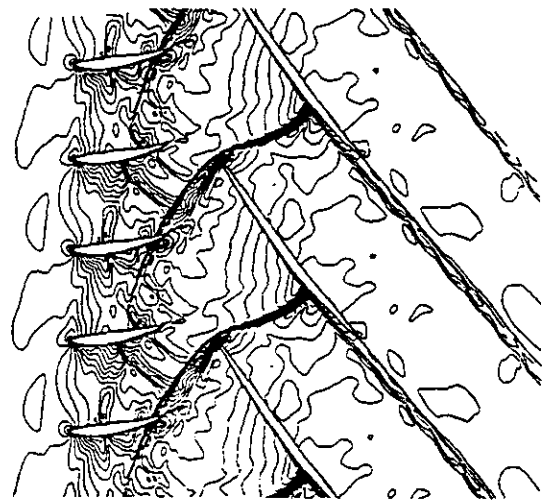

B

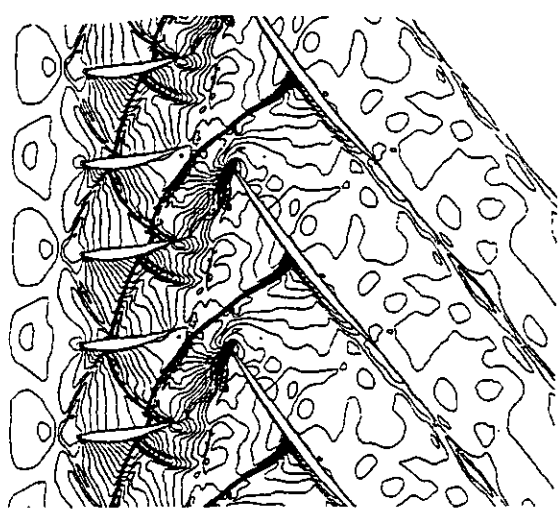

C

FIG. 4, INSTANTANEOUS DENSITY CONTOURS FOR CHOKE (A), PEAK EFFICIENCY (B), AND NEAR STALL (C) CONDITIONS.

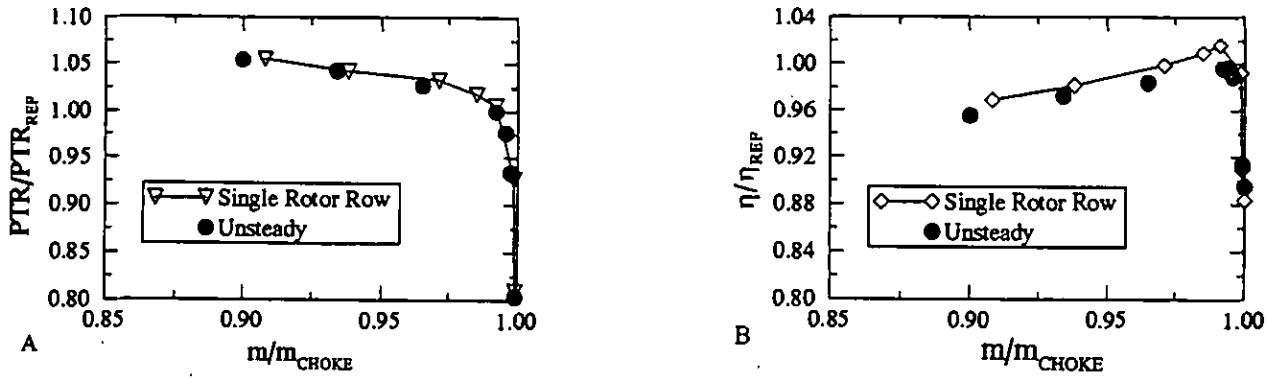

FIG. 5, COMPARISON BETWEEN UNSTEADY AND STEADY SINGLE ROTOR ROW RESULTS IN TERMS OF TOTAL PRESSURE RATIO (A), AND ADIABATIC EFFICIENCY (B).

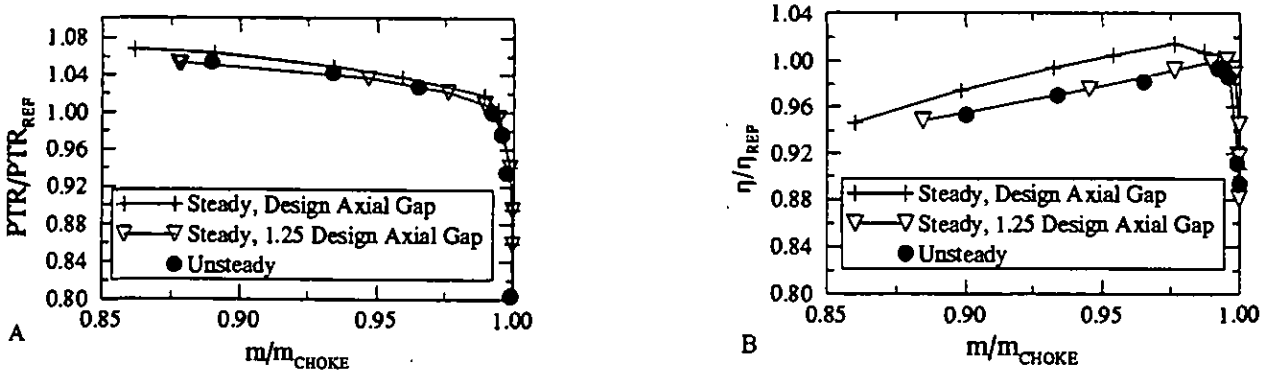

FIG. 6, EFFECTS OF THE AXIAL GAP BETWEEN ROWS ON STEADY TOTAL PRESSURE RATIO (A), AND ADIABATIC EFFICIENCY (B) FOR THE ONE-DIMENSIONAL CHARACTERISTIC BOUNDARY TREATMENT

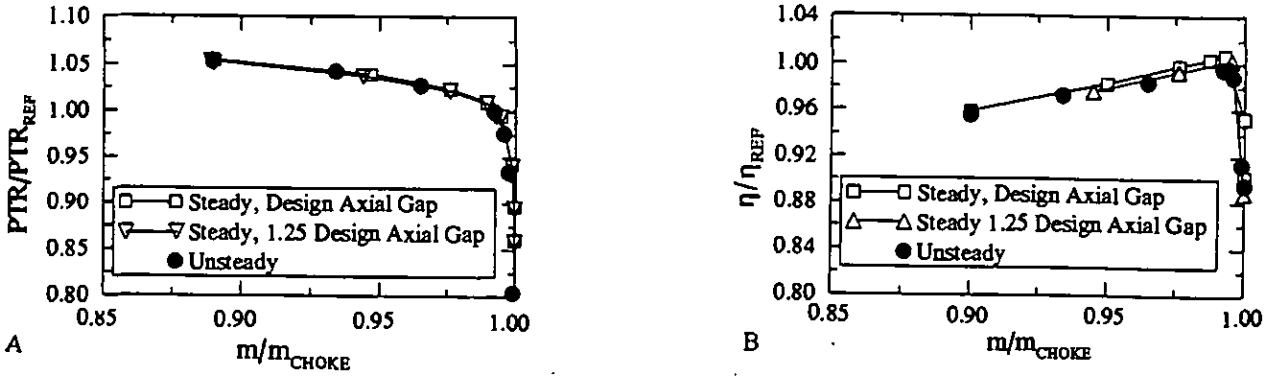

FIG. 7, EFFECTS OF THE AXIAL GAP BETWEEN ROWS ON STEADY TOTAL PRESSURE RATIO, (A), AND ADIABATIC EFFICIENCY (B) FOR NON-REFLECTIVE BOUNDARY CONDITIONS.

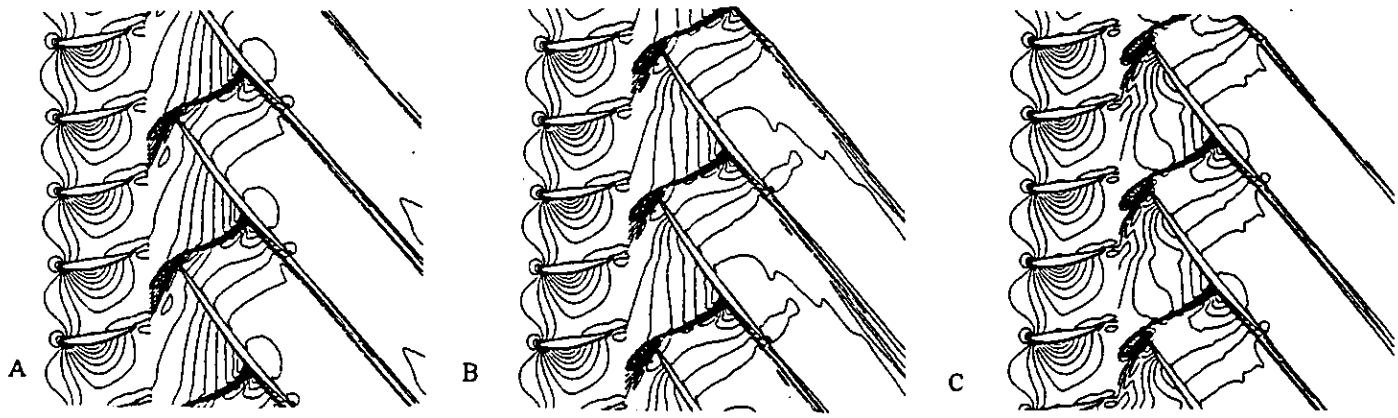

FIG. 8, DENSITY CONTOURS FOR TIME-AVERAGED SOLUTION (A), STEADY SOLUTION WITH NON-REFLECTIVE BOUNDARY CONDITIONS (B), AND STEADY SOLUTION WITH ONE-DIMENSIONAL CHARACTERISTIC TREATMENT (C).

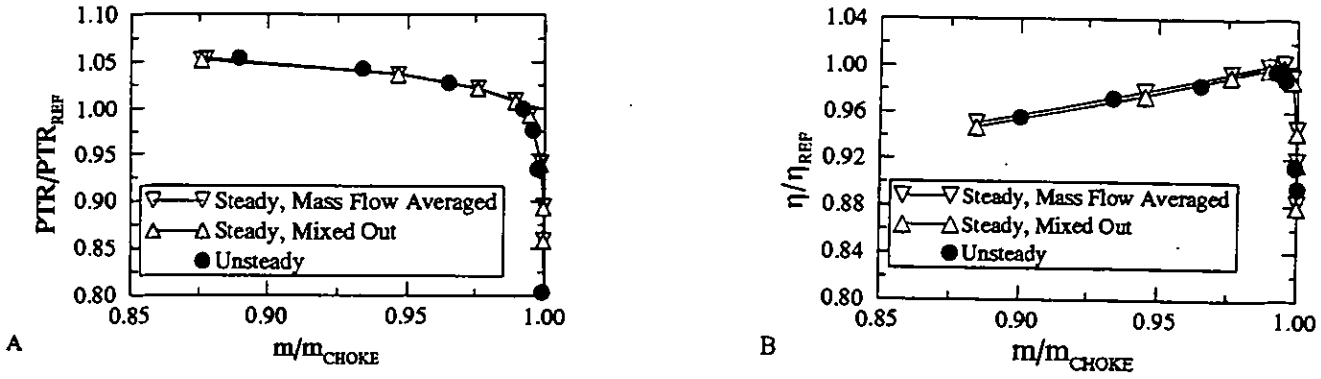

FIG. 9, EFFECT OF THE INTERFACE PITCH-AVERAGING ON STEADY TOTAL PRESSURE RATIO (A), AND ADIABATIC EFFICIENCY, (B).